

# Aeroacoustic effects of a cylinder/plate-configuration

Michael Winkler\* and Klaus Becker†

*Cologne University of Applied Sciences, Cologne, 50679, Germany*

Con Doolan‡

*The University of Adelaide, Adelaide, South Australia, 5005, Australia*

Frank Kameier§

*University of Applied Sciences Düsseldorf, Düsseldorf, 40474, Germany*

Christian Oliver Paschereit¶

*Technical University of Berlin, Berlin, 10623, Germany*

The interaction of bluff bodies in an air flow can generate high sound pressure levels. Especially for the interaction of the cylinder/plate-configuration the generated noise can be amplified enormously by the insertion of a plate behind a cylinder. In this work the aeroacoustic sound generation of a cylinder/plate-configuration has been investigated experimentally. The amplification of the generated sound is quantized and the condition for the amplification is analyzed in detail. In the experiments the distance between cylinder and plate as well as the flow velocity were varied. A critical spacing that depends on the flow velocity was found, for which the sound pressure levels rise dramatically. The variation of the distance and the flow velocity also showed a hysteresis effect regarding the occurrence of the sound pressure amplification.

## Nomenclature

$d$	cylinder diameter, mm
$g$	cylinder-plate distance, mm
$t$	plate thickness, mm
$u$	flow velocity, m/s
$St_c$	Strouhal number single cylinder, -
$St_{c+p}$	Strouhal number cylinder/plate-configuration, -
$p_c$	sound pressure single cylinder, Pa
$p_{c+p}$	sound pressure cylinder/plate-configuration, Pa
$V$	amplification factor, -
$C_s$	sound pressure coefficient, -
$C_L$	sectional r.m.s. lift coefficient, -
$\Lambda$	correlation length, mm

## I. Introduction

The sound generation by bodies immersed in an airstream is important for a wide range of industrial applications like air conditioning systems, wind turbines or heat exchangers. This holds especially for aero-

---

\*Scientific Assistant, Institute of Automotive Engineering, Betzdorfer Strasse 2.

†Professor, Institute of Automotive Engineering, Betzdorfer Strasse 2.

‡Senior Lecturer, School of Mechanical Engineering, Senior Member, AIAA.

§Professor, Fachbereich Maschinenbau und Verfahrenstechnik, Josef Gockeln Strasse 9.

¶Professor, Chair of Fluid Dynamics - Hermann-Föttinger-Institute (HFI), Müller-Breslau-Strasse 8.

nautic applications such as landing gears for example. Further, the sound generation by the interaction of bluff bodies can be enhanced enormously under certain circumstances. A deep knowledge of the underlining sound generation mechanisms is therefore important.

The interest of bluff body interactions for aeroacoustics can be seen by the high number of publications on this field of research. A widely used setup is the combination of cylinders and airfoils. The experiments of Jacob et. al.<sup>6</sup> provide interesting physical information about a rod-airfoil configuration. At subcritical Reynolds numbers, the instantaneous flow field is quite different from the classical vortex street. Strong three-dimensional effects, secondary vortices, vortex splitting, and stretching significantly distort the flow field and are responsible for spectral broadening around the shedding frequency and its harmonics. They are particularly strong near the leading edge. As a result, the leading edge is the dominant source region. Greschner et. al.<sup>4</sup> predict the unsteady flow field generated by an airfoil in the wake of a circular rod numerically by using a Detached-Eddy Simulation (DES) and use a Ffowcs Williams and Hawkins acoustic analogy formulation for the computation of far field sound. Kao<sup>7</sup> numerically investigated the sound generation of vortices interacting with an arbitrary body in a low-speed flow by the method of matched asymptotic expansions. Kao concluded that sound radiation from vortex/bluff-body interactions is almost always lower than that from the vortex/airfoil interaction. The explanation lies perhaps in the flow pattern in the nose region of a bluff body, where the fluid, after impacting a flat surface, branches off into two streams and skirts the corners to be away from the body. As a result, the vortex never gets a chance to be very close to the surface, and there is less interaction.

Other interesting phenomena regarding the interaction of bluff bodies are hysteresis effects. Many investigators study the interaction of flexible bodies or flexible mounted bodies which show hysteresis regarding the vibration behavior and the flow pattern (Singh et. al.,<sup>16</sup> Brika et. al.,<sup>1</sup> Wanderley et. al.<sup>18</sup>). Also, the interaction of rigid bodies experiences hysteresis effects, even if there are fewer publications. Liu and Chen<sup>10</sup> for example study a configuration of two square cylinders in tandem arrangement. It is shown, that the flow patterns are not only affected by the distance of the bodies. They depend on the manner in which the distance is varied. Tasaka et. al.<sup>17</sup> investigate two circular cylinders in tandem arrangement and visualize the flow pattern. According to how the distance is changed, two different flow modes are discerned. Carmo et. al.<sup>2</sup> also investigate the possible states in the flow around two identical circular cylinders in a tandem arrangement. Numerical simulations are used to study the hysteresis in the transition region of flow modes. The relationship between three dimensional instabilities and hysteresis is also addressed.

In the before mentioned investigations on hysteresis effects only the interaction of equal shaped bodies are investigated and acoustics are not considered. The aim of this investigation is to enhance the knowledge of physical effects like the hysteresis for two different interacting bodies and their impact on the aeroacoustic sound generation mechanisms. Therefore a simple configuration is chosen, which consists of a circular cylinder and a flat plate. The main issue of the present investigation is sound amplification, caused by placing the plate in the wake of the circular cylinder. The prerequisites for the sound amplification are analyzed by varying the spacing between the bodies and the flow velocity. Hysteresis effects regarding the variation of these parameters are investigated and the amplification is quantified in relation to the Reynolds number.

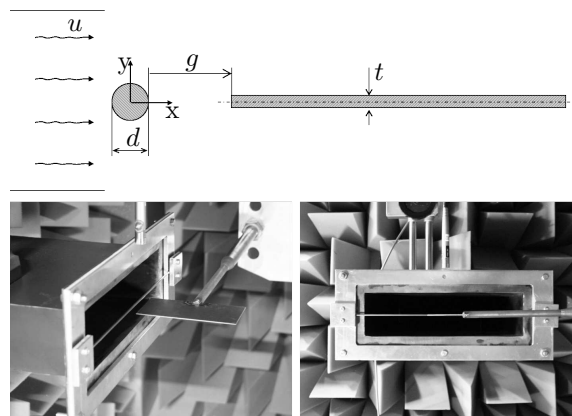


**Figure 1. Schematic representation of the test setup (top); photographs of the test setup (bottom).**

## II. Experimental setup

The experiments are carried out in the University of Adelaide's anechoic wind tunnel, where a free jet is generated at a rectangular channel outlet (275 x 75 mm). The turbulence intensity, measured in the center of the outlet plane is 0.4%. The test configuration consisting of a flat plate and a circular cylinder is placed in the core of a free jet (Figure 1). The plate with its dimensions of 120 x 60 x 1 mm is made out of steel. It is supported by a steel rod, which is mounted to a computer controlled traverse system. The mainly used cylinder diameter  $d$  is 3 mm, but there are also measurements where the cylinder diameter was varied from 2 mm up to 10 mm. The maximum flow velocity  $u$  is 30 m/s. It is calculated out of pressure measurements by a pitot tube, which is mounted in the center of the outlet plane preliminary to the tests. Based on cylinder diameter and maximum velocity the Reynolds number is up to about  $1.7 \times 10^4$  and the Mach number is below 0.09. Acoustic data are acquired by an half inch condenser microphone. The microphone is placed perpendicular to the cylinder axis at half height of the test configuration in 0.08 m distance from the center.

## III. Results

### A. Comparison of configurations

The auto power spectra of the sound pressures for different test configurations at a flow velocity of 15 m/s is shown in Figure 2. Additional to the results of the cylinder/plate-configuration the results of the free jet, the plate, the cylinder as well as the no-flow background noise are plotted for reference. The background noise measurement shows, that there are some external disturbances in the frequency range around 200 Hz. However, the signal to noise ratio is big enough to avoid an influence of this disturbances on the measurement results of the test configurations. By the noise measurements of the free jet it can be seen that the sound pressure level below 300 Hz is mainly caused by the free jet. Only the single plate and the cylinder/plate-configuration generate additional noise around a frequency of approximately 200 Hz. This noise is generated by vortices shedding from the rod supporting the plate. The insertion of the plate into the free jet also

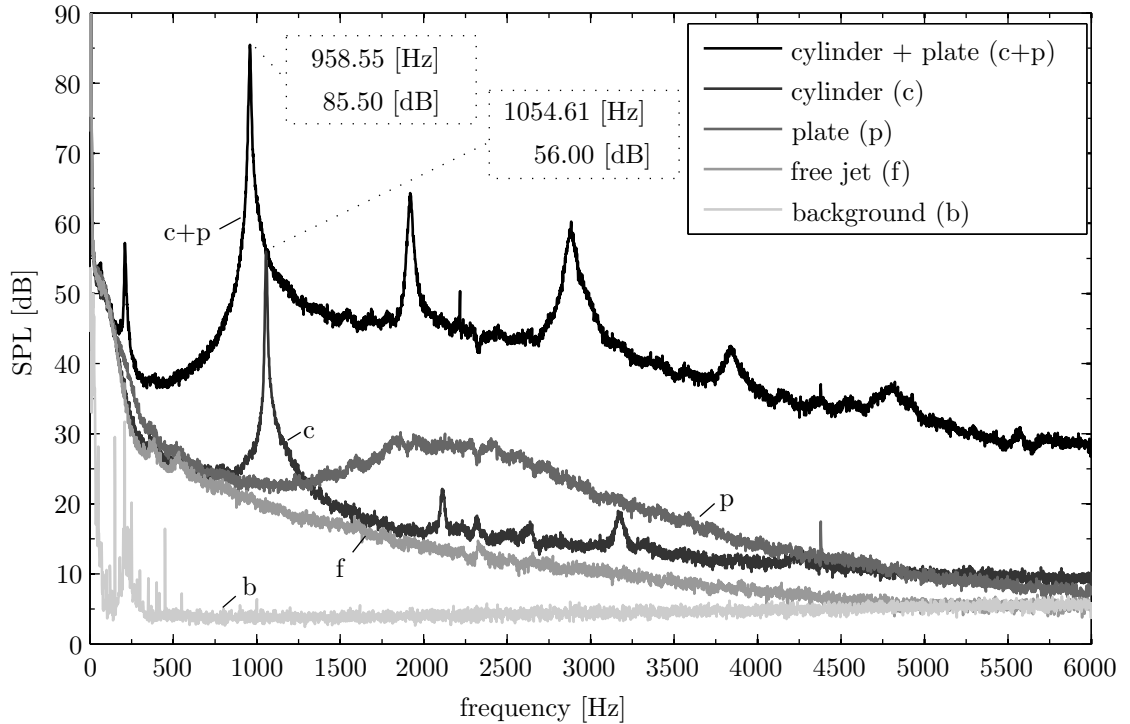


**Figure 2.** Auto power spectra of the sound pressure levels for different test configurations. Normalized distance  $g/d = 4$ ; flow velocity  $u = 15$  m/s; Reynolds number  $Re = 2250$ .

causes an increase of the sound pressure level between 1 000 Hz and 4 000 Hz with broadband characteristic. In comparison to the results for the single plate, the single cylinder within the free jet produces an increase of the sound pressure level centered on 1 055 Hz. This behavior is caused by alternately shedding vortices from the cylinder and by the vortex street behind the cylinder. The resulting Strouhal number is 0.21, as to be expected for a circular cylinder at a Reynolds number of 3 000. Furthermore first and second harmonics are visible. The additional positioning of the plate in the wake of the cylinder causes a large amplification of the sound pressure level. The sound pressure level increases by nearly 30 dB, which is a factor of around 30 in the linear scale. The harmonics are amplified even more as it can be seen by additional occurring harmonics. There is also a change in frequency. In comparison to the single cylinder the main peak for the cylinder/plate-configuration decreases to 959 Hz. This results in a value of 0.19 for the Strouhal number. The investigation of the frequency behavior is part of this research and will be discussed later in this article. The main focus of this investigation is on the conditions for the amplification of the sound pressure level according to the spacing between the cylinder and the plate as well as the flow velocity.

## B. Parameter variations

The results for the parameter variations were acquired by setting the flow velocity and then increasing the normalized distance  $g/d$  from 0 to 5. This procedure is repeated for each flow velocity between 0 and 30 m/s with a resolution of 0.3 m/s. The resolution of the distance variation is 0.25 mm. That results in 6 161 measurement points and gives a detailed overview of the system behavior (Figure 3). There are two regions to be differentiated. Below a normalized distance of around 2.75 the overall sound pressure level is significantly lower than for bigger distances. In that region the cylinder-plate/configuration generates less noise because the plate acts like a so called splitter plate and avoids the generation of vortices behind the cylinder. These results match with findings in literature, that there is a critical spacing between normalized distances of 2 to 3. But to the authors knowledge, there are fewer investigations on the dependency of the critical spacing on the flow velocity respectively the Reynolds number in that detail and in consideration of the impact on aeroacoustics.

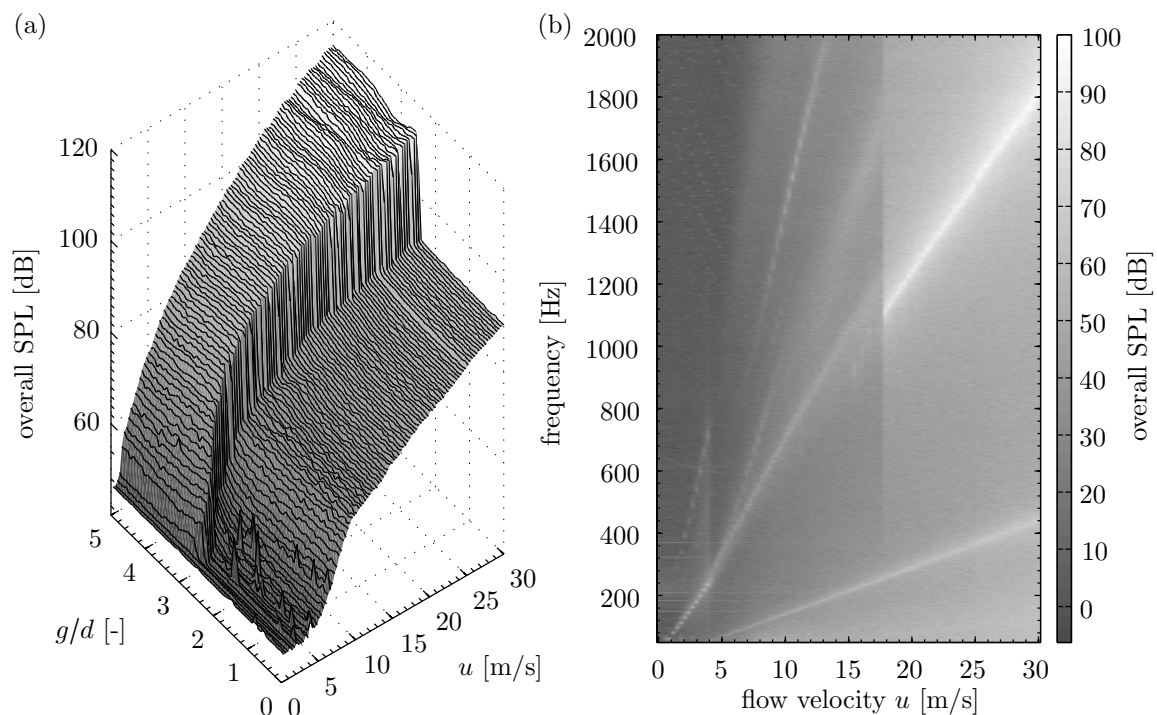
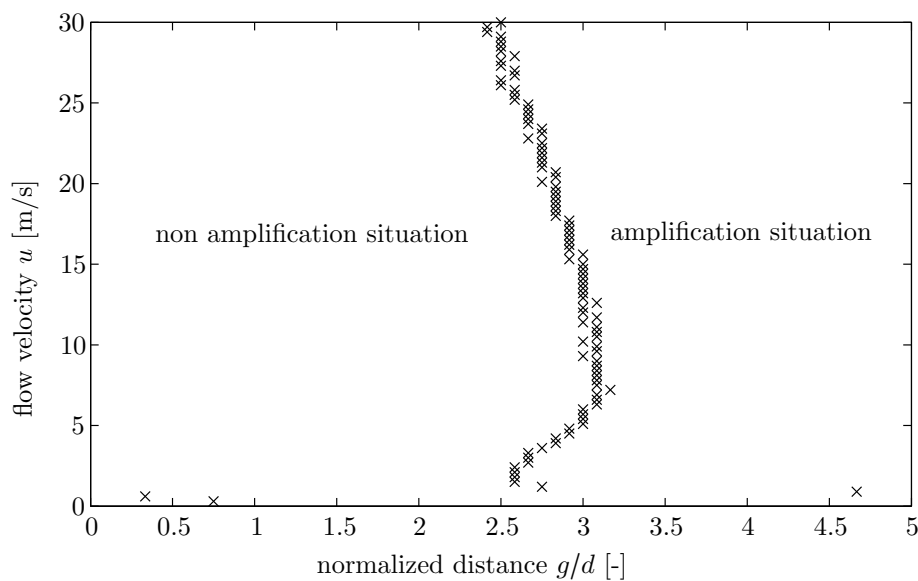


Figure 3. Overall sound pressure level, bandpass filtered between 50 Hz and 12 800 Hz, of the cylinder/plate-configuration for variation of normalized distance  $g/d$  and flow velocity  $u$ . (a) Overview of all measurement points, (b) spectrogram for a normalized distance  $g/d = 2.9$ .

The spectrogram on the right hand side of Figure 3 provides an insight into the behavior of the investigated configuration. The diagram contains the sound pressure level spectra of all tested flow velocities at a normalized distance of 2.9. The data show some areas of sound pressure level rise, for which the relation between frequency and velocity is approximately linear. The line of sound pressure level rise below 400 Hz, which shows up over the whole velocity range, is caused by shedding vortices from the support of the plate. The support consists of a cylindrical rod with a diameter of 11 mm and is therefore expected to produce sound at relative low frequencies compared to the tested cylinder with its 3 mm diameter. Because of its low frequency content and the relative low sound pressure levels compared to the amplified sound pressure levels, the influence of the support on the investigated effects can be neglected. The actual region of interest in the spectrogram spans from the left bottom corner of the diagram to the right upper corner. For flow velocities below 4 m/s and frequencies less than 250 Hz the sound pressure level of the cylinder/plate-configuration is amplified. The rise can also be seen by the additional occurring first harmonic at the double of the frequencies. For a further increase of the flow velocity the sound pressure amplification vanishes. The still existing line of sound pressure rise between 4 m/s and 18 m/s has a different gradient and is less intense. It is produced by vortices still shedding from the outer parts of the cylinder, where the plate is not behind it (see Figure 1). At 17.9 m/s and a frequency of around 1 100 Hz the sound pressure level increases drastically. It can be seen, that the sound pressure level rises over the whole frequency range and at most at the vortex shedding frequency. In addition to that, the vortex shedding frequency drops by around 100 Hz.

The diagram in Figure 4 is created out of the measurement results shown in Figure 3. The illustrated points



**Figure 4. Critical spacing for transition from non-amplification to amplification situation, marked by  $\times$  at biggest sound pressure level rise of data in Figure 3.**

mark the change between the amplification and non-amplification situation as a function of flow velocity and normalized distance. It can be seen that the critical distance depends on the flow velocity respectively the Reynolds number. At relatively high flow velocities the critical distance decreases approximately linearly with the flow velocity and approaches a maximum. This maximum value of 3.2 in terms of normalized distance  $g/d$  is reached for a flow velocity of around 6 m/s ( $Re = 1\,200$ ). Interestingly, below this velocity the critical distance, at which the sound pressure level is amplified, reduces again. An explanation for this effect can be found in the literature. Norberg<sup>12</sup> investigates the vortex formation length for a flow around a single circular cylinder and for varying Reynolds numbers. From these results and according to measurement results of other researches, it can be seen that the vortex formation length has a maximum at a Reynolds number of about 1 200 and decreases for lower and higher Reynolds numbers. There is a slight difference between the absolute values of formation length and the critical spacing of the present investigation. This difference might be attributed to slight changes in the formation of the cylinder wake because of the downstream plate. An

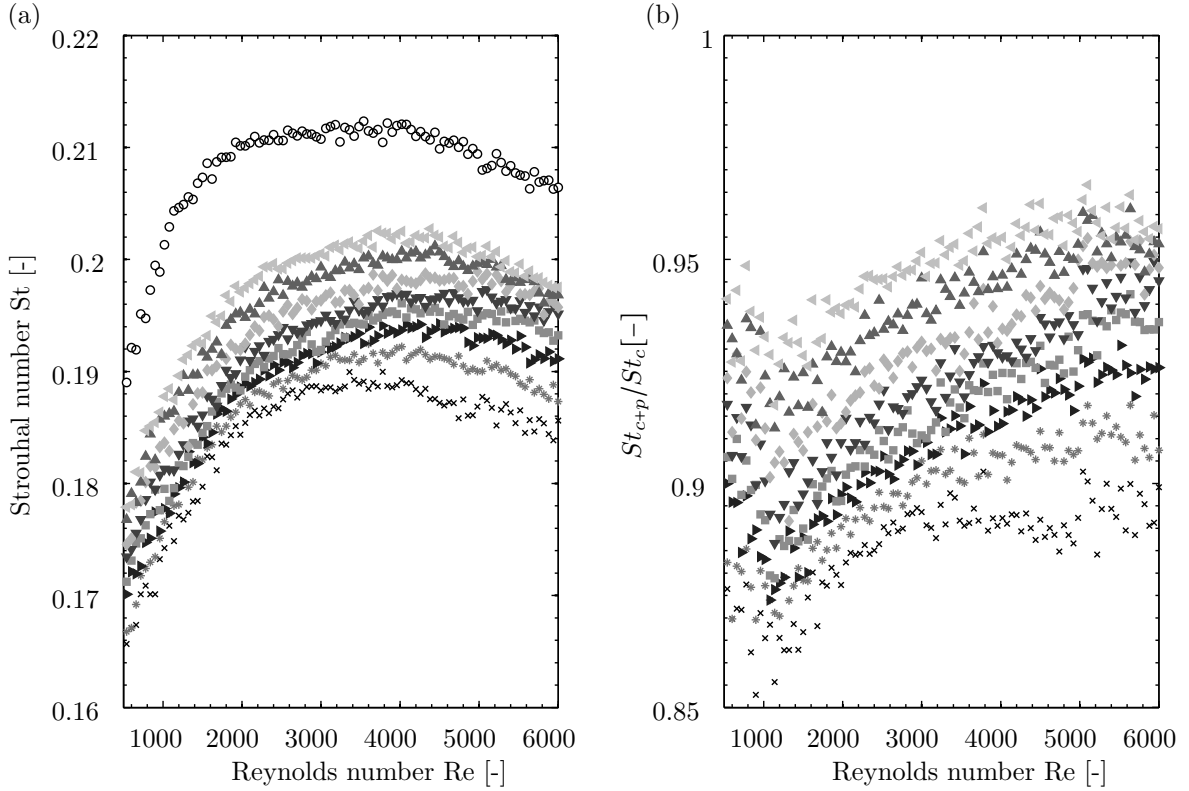


**Figure 5.** (a) Strouhal number as a function of Reynolds number for single cylinder  $\circ$ , and different normalized distances  $g/d = 3.17, \times$ ;  $3.42, *$ ;  $3.67, \triangleright$ ;  $3.92, \square$ ;  $4.17, \blacktriangleright$ ;  $4.42, \blacklozenge$ ;  $4.67, \blacktriangle$ ;  $4.92, \blacktriangleleft$ , (b) Strouhal number reduction of cylinder/plate-configuration  $St_{c+p}$  in relation to the Strouhal number for the single cylinder  $St_c$ .

indication for this is the frequency variation as discussed for the results in Figure 2. But in general it can be seen, that the critical distance for the sound pressure level amplification of the cylinder/plate-configuration is linked to the vortex formation length of the cylinder wake.

### C. Frequency behavior

The relation of shedding frequency, flow velocity and normalized distance  $g/d$  can be seen by Figure 5. Here the Strouhal number is plotted against the Reynolds number for values of  $g/d$  from 3.17 to 4.92. For that region of distances the sound pressure amplification and with this also the alteration of the vortex shedding frequency exists over the whole velocity and Reynolds number range respectively. Additional to that, the result for the single cylinder is plotted. The dependency of Strouhal number and Reynolds number for the single cylinder can be differentiated in three regions by the shape of the curve. Between Reynolds numbers from 500 to approximately 1 250 the Strouhal number shows a steep and nearly linear increase. For higher Reynolds numbers up to 3 900 the Strouhal number increases further, but the inclination is not linear anymore. From Reynolds numbers of 3 900 onwards the Strouhal number starts to decrease again in a linearly manner. The changes in the run of the curve are attributed to changes in the pattern of the vortex street, as it is discussed by Roshko<sup>15</sup> and Fey et. al.<sup>3</sup> for example. The curves for the cylinder/plate-configurations show a likewise behavior although the changes are not that well pronounced. The gap between single cylinder result and cylinder/plate-configurations shows the drop of the vortex shedding frequency caused by the insertion of the plate behind the cylinder. It can be seen, that the drop of Strouhal number is smallest for the biggest distance between cylinder and plate. The nearer the plate approaches the cylinder, the more the vortex shedding process is altered. On the right hand side of Figure 5 the Strouhal numbers of the cylinder/plate-configurations are related to the single cylinder case. It can be seen that the reduction of Strouhal number depends on the Reynolds number as well. The reduction is biggest at Reynolds numbers of around 1 250. For increasing Reynolds numbers the difference reduces. As discussed in subsection B the

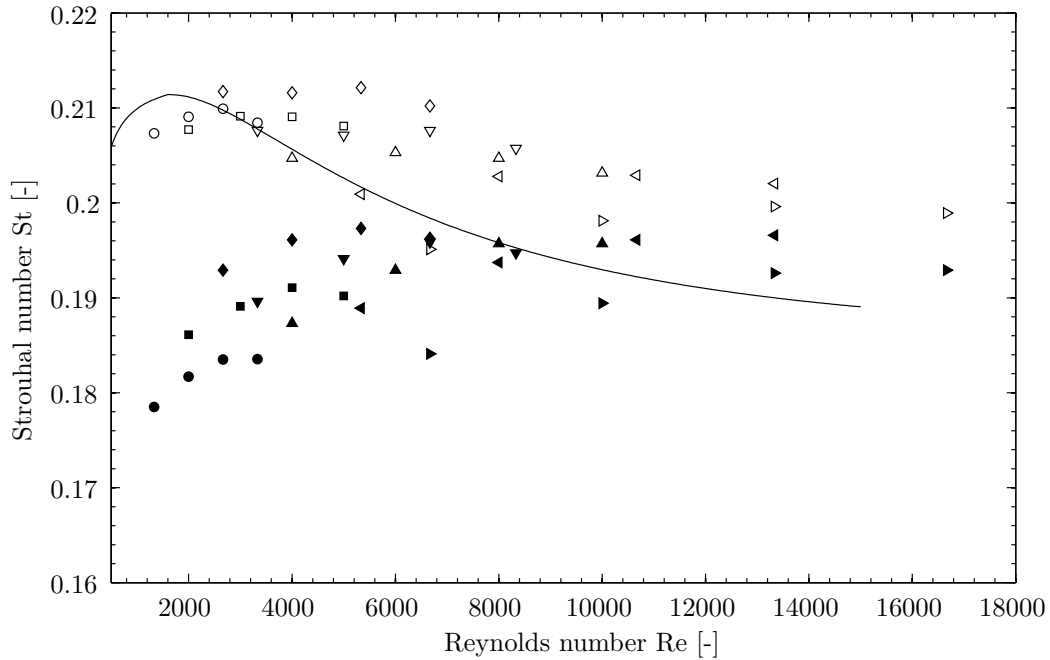


Figure 6. Strouhal number as a function of Reynolds number for the single cylinder (empty symbols) and the cylinder/plate-configuration (filled symbols) at  $g/d=4$ . The Reynolds number is varied by four different flow velocities, 10 m/s, 15 m/s, 20 m/s, 25 m/s and seven cylinder diameters. 2 mm,  $\circ$ ,  $\bullet$ ; 3 mm,  $\square$ ,  $\blacksquare$ ; 4 mm,  $\diamond$ ,  $\blacklozenge$ ; 5 mm,  $\nabla$ ,  $\blacktriangledown$ ; 6 mm,  $\triangle$ ,  $\blacktriangle$ ; 8 mm,  $\triangleleft$ ,  $\blacktriangleleft$ ; 10 mm,  $\triangleright$ ,  $\blacktriangleright$ ; empirical formula of Norberg<sup>13</sup>, - .

length of the vortex formation region is reduced for increasing Reynolds numbers higher than 1250. Because of this the effective distance between the leading edge of the plate and formation region increase although the normalized distance is kept constant. Therefore the influence of the plate on the vortex shedding process is less intense and the Strouhal number increases towards the value of the single cylinder.

This behavior can also be seen in Figure 6. Here the Strouhal/Reynolds number relation is shown for a range of Reynolds numbers from 500 up to  $1,8 \times 10^4$ . The wide range of Reynolds numbers is set by varying the flow velocity from 10 m/s to 25 m/s in increments of 5 m/s and the use of different cylinders with 2, 3, 4, 5, 6, 8 and 10 mm in diameter. The measurements are taken for the single cylinder case (empty symbols) and the cylinder/plate-configuration (filled symbols) for a fixed normalized distance  $g/d=4$ . Additional to that an empirical function by Norberg<sup>13</sup> for the Strouhal number of a circular cylinder is plotted for reference. The measurement data show some scatter for equal Reynolds numbers. One reason for the scatter might be the changing aspect ratio of cylinder diameter and cylinder length, which is 17.5 for the biggest cylinder and 77.5 for the smallest cylinder. One can expect the flow at around mid-span to be effectively decoupled from the Strouhal number influencing end effects at some finite aspect ratio. Norberg<sup>11</sup> suggests a minimum aspect ratio of around 50 for  $600 < Re < 4000$  and 60-70 for  $4000 < Re < 10^4$ . The effect of outlet area blockage on the flow velocity by the cylinders is corrected by means of experimentally determined correction factors. The run of the curve of the measurement data for the single cylinder case in general agree with the empirical function of Norberg. Presumably the disparity between the present results and those of Norberg are combination effects related to the notable differences in end conditions of the cylinder, turbulence level and aspect ratio. The comparison of the single cylinder case with the results for the cylinder/plate-configuration show the biggest difference for small Reynolds numbers. For increasing Reynolds numbers the difference is reduced. At very high Reynolds numbers of around  $10^4$  the difference is nearly constant. This complies with the argumentation in the last paragraph. The vortex formation length also reaches a nearly constant value in this range of Reynolds numbers and with this the influence of the plate on the vortex formation process stays unchanged.

#### D. Hysteresis effects

After the dependency of the vortex shedding frequency on the normalized distance and the Reynolds number has been investigated in detail, another question arises from the results in literature discussed in the introduction. There are hysteresis effects reported regarding vibrational behavior and flow patterns. The question is, whether the sound pressure amplification of the cylinder/plate-configuration not only depends on the normalized distance and the flow velocity, but also on the manner in which the parameters are varied. For this investigation, the flow velocity is set to 12 m/s and the distance is increased by 0.25 mm steps from 0 to 15 mm, which corresponds to a normalized distance of 0 to 5. After this, the plate is moved backwards to zero distance. The results of these measurements are shown in Figure 7. The overall sound pressure level is bandpass filtered between 50 Hz and 12800 Hz. It is plotted as a function of the normalized distance  $g/d$ . The points acquired for the increasing distance jump from one state to the other at a normalized distance of nearly 3.2. For the decreasing distance there is no drop back to the non-amplified state until a value of 2.7. The results show a hysteresis effect for the variation of the distance. In the region between the normalized distances of 2.7 to 3.2 the non-amplified as well as the amplified state could be stable depending on the direction of parameter variation.

The dependency of the sound pressure level amplification on the manner of flow velocity variation is ana-

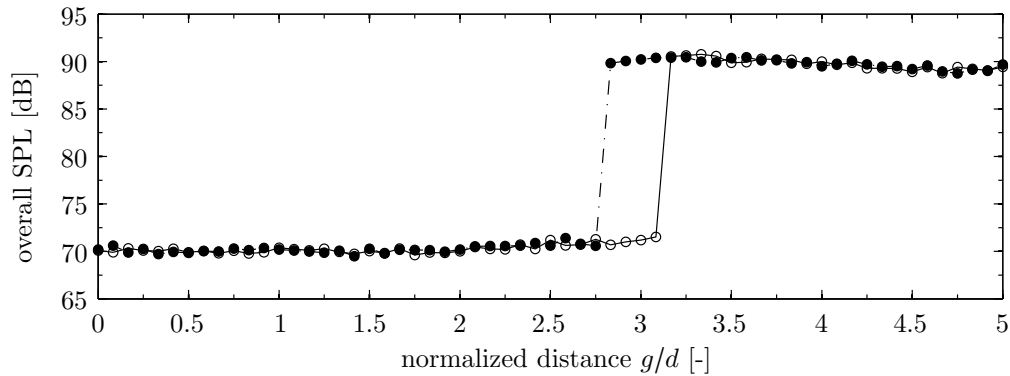


**Figure 7.** Distance-hysteresis of the overall sound pressure level for flow velocity  $u = 12$  m/s; increased distance,  $\circ$ ; decreased distance,  $\bullet$ .

lyzed for constant values of normalized distance. The flow velocity is increased from 0 to 24 m/s, in 0.3 m/s steps and then decreased to zero velocity again. The results of these measurements can be seen from Figure 8. The overall sound pressure level is plotted against the flow velocity for three different distances. In the upper diagram the normalized distance is set to 2.75, which corresponds to a distance of 8.25 mm. The sound pressure amplification exists right from the beginning at low flow speeds. It then vanishes for slightly higher velocities and occurs again at a much higher flow speed. If the flow velocity is decreased again, the sound pressure amplification vanishes at a lower flow velocity compared to the establishing for increasing velocity. The same effect exists for the change at lower flow speeds. The diagram in the middle of Figure 8 is plotted for a normalized distance of 3. The comparison of increased and decreased flow velocity variation show the same hysteresis effect like for a distance of  $g/d = 2.75$ , although the changes occur at different flow speeds. The lower diagram shows the results for a normalized distance of 3.25. These measurement results do not show any great change of the sound pressure level. The sound pressure amplification is stable for all flow speeds. All results in Figure 8 match well with the findings in Figure 3 and they show an additional aspect of the flow velocity variation. The occurrence of sound pressure level amplification for the cylinder/plate-configuration does not only depend on the flow velocity variation, it also depends on the manner in which the velocity is varied.

#### E. Quantification of the sound pressure amplification

In the previous subsections the specific conditions under which the sound pressure is amplified by the plate are discussed in detail. The concern of the following subsection is to quantify the amplification of the

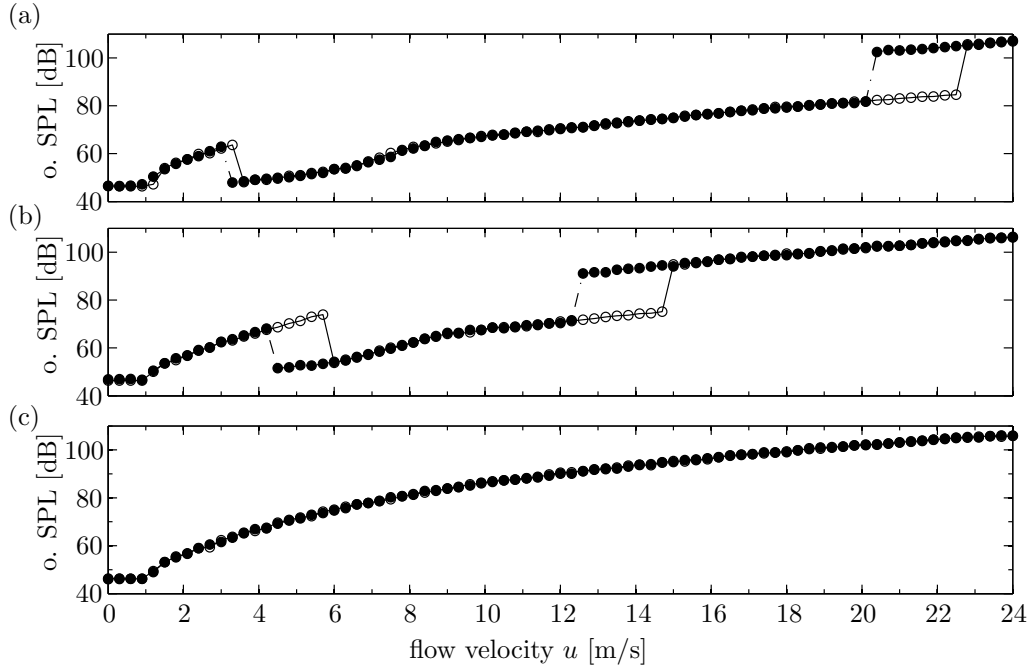


Figure 8. Flow velocity-hysteresis of the overall sound pressure level for three different normalized distances; increased distance,  $\circ$ ; decreased distance,  $\bullet$ ; (a)  $g/d = 2.75$ ; (b)  $g/d = 3$ ; (c)  $g/d = 3.25$ .

cylinder/plate-configuration in comparison with the single cylinder case. Therefore an amplification factor  $V$  is defined.

$$V = \frac{p_{c+p}}{p_c} \quad (1)$$

In this definition  $p_{c+p}$  is the sound pressure of the cylinder/plate-configuration and  $p_c$  that of the single cylinder, taken at the corresponding vortex shedding frequencies. The dependency of the amplification factor on the flow velocity is plotted in Figure 9. The results are shown for measurements taken with a cylinder of 3 mm in diameter and a normalized distance  $g/d = 4$ . The results for this normalized distance are plotted for instance. The run of the curve is similar for all the normalized distances between 3.17 and 4.92 which result in the sound pressure amplification over the whole velocity and Reynolds number range respectively. The Reynolds number is altered by variation of the flow velocity.

For a Reynolds number of 500 the amplification factor starts to increase from values of around 10 to 15 up to 40 for a Reynolds number of 1500. Irrespective a small reduction of the amplification factor at around a Reynolds number of 2300,  $V$  varies between 25 to 40 for the range between Reynolds numbers of 1500 and 3900. From there on the amplification factor decreases to a value of 7 at  $Re = 6000$ . The reason for the decrease of the amplification factor for higher Reynolds numbers is investigated by means of Figure 10. Here the sound pressure level of the cylinder/plate-configuration and the single cylinder are plotted as a function of the Reynolds number. The sound pressure levels are scaled by subtraction of the logarithm of the flow velocity to the power of 5.3. Hence a horizontally run of a curve denotes that the radiated power is proportional to  $u^{5.3}$ . The cylinder/plate-configuration shows this behavior for Reynolds numbers higher than  $Re = 2000$ . For lower Reynolds numbers the value is less than 5.3. The behavior of the single cylinder can be differentiated in three regions as follows. Below Reynolds numbers of 1250 the exponent of the flow velocity is much lower than 5.3. Between Reynolds numbers of approximately 1250 and 3000 the sound pressure level of the single cylinder behaves like the cylinder/plate-configuration and varies with  $u^{5.3}$ . For Reynolds numbers above 3000 the single cylinder shows a different behavior. The exponent of the flow velocity is much higher than 5.3 as to be seen by the steeply increase of the scaled sound pressure level.

The amplification factor is roughly constant in the Reynolds number range between 1250 and 3000. This is caused by the nearly similar proportionality of the flow velocity and the radiated sound power for the cylinder/plate-configuration and the single cylinder. The drop of the amplification factor for higher Reynolds

numbers is caused by the single cylinder. The proportionality of radiated power and flow velocity rises compared to the cylinder/plate-configuration. Hence, the radiated power increase faster with the Reynolds number for the single cylinder in comparison to the cylinder/plate-configuration and therefore the amplification factor drops.

The reason for the change in sound power radiation by a cylinder can be found in the dependence of the sound power radiation on the lift coefficient. The noise radiated by a cylinder with vortex shedding is closely related to its lift coefficient, as can be seen in the theory of Phillips<sup>14</sup> for example. A sound pressure coefficient  $C_s$  is defined by Keefe<sup>8</sup> in terms of sectional r.m.s. lift coefficient  $C_{L'}$ , Strouhal number  $St$  and normalized spanwise correlation length  $(\Lambda/d)$ .

$$C_s = C_{L'} St \sqrt{\Lambda/d} \quad (2)$$

Deviations from a sixth-power law as it is normally expected for a dipole sound source like the vortex shedding cylinder (see Heckel<sup>5</sup>) will occur when  $C_s$  varies with the Reynolds number. By combination of measurement data from several different authors Norberg<sup>13</sup> shows that the sound pressure coefficient strongly depends on the Reynolds number. For Reynolds numbers between 3 000 and 6 000 the sound pressure coefficient rapidly increases. The measurement data of Leehey and Hanson<sup>9</sup> support the rapid increase and their sound pressure measurements also show significant deviations from a sixth-power law.

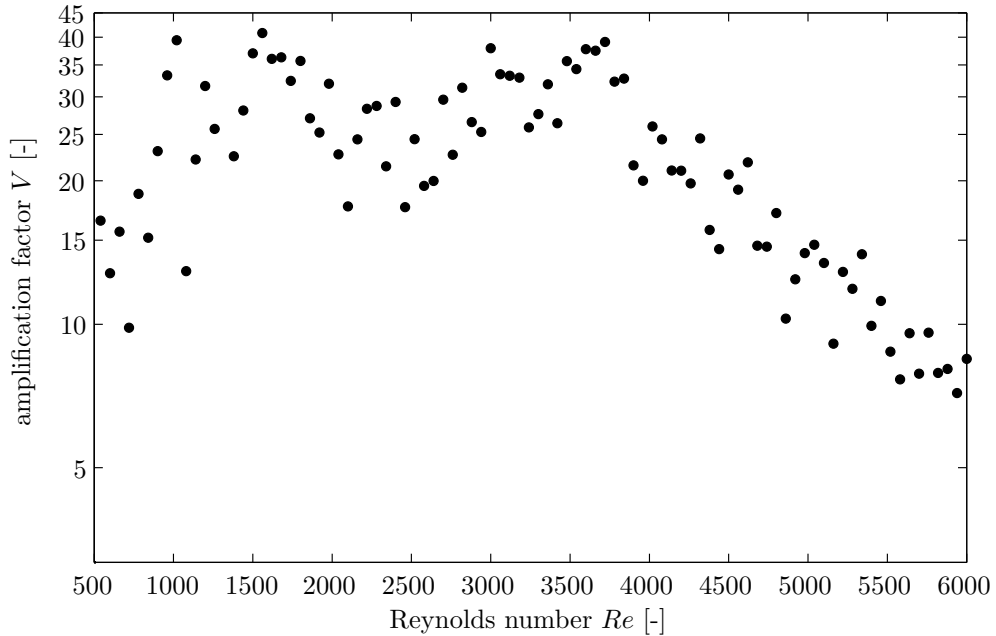


**Figure 9.** Amplification factor as a function of flow velocity. Cylinder diameter  $d = 3$  mm, normalized distance  $g/d = 4$ .

## IV. Conclusion

Aeroacoustic effects regarding the flow around a circular cylinder and a downstream flat plate have been investigated experimentally. Compared with the single cylinder case, the positioning of the plate behind the cylinder can amplify the generated sound pressure. The occurrence of this sound pressure amplification depends on the flow velocity as well as the distance between cylinder and plate. It also depends on the manner in which the parameters are varied. The results for the variation of flow velocity as well as the variation of distance between cylinder and plate show hysteresis regarding the occurrence of the sound pressure amplification. This sound pressure rise can be quantified by a factor  $V$ , which is around 30 for lower Reynolds numbers and decreases for increasing Reynolds numbers. The Strouhal number is reduced by the insertion of the plate in relation to its position. The influence of the plate on the Strouhal number reduces for increasing Reynolds numbers.

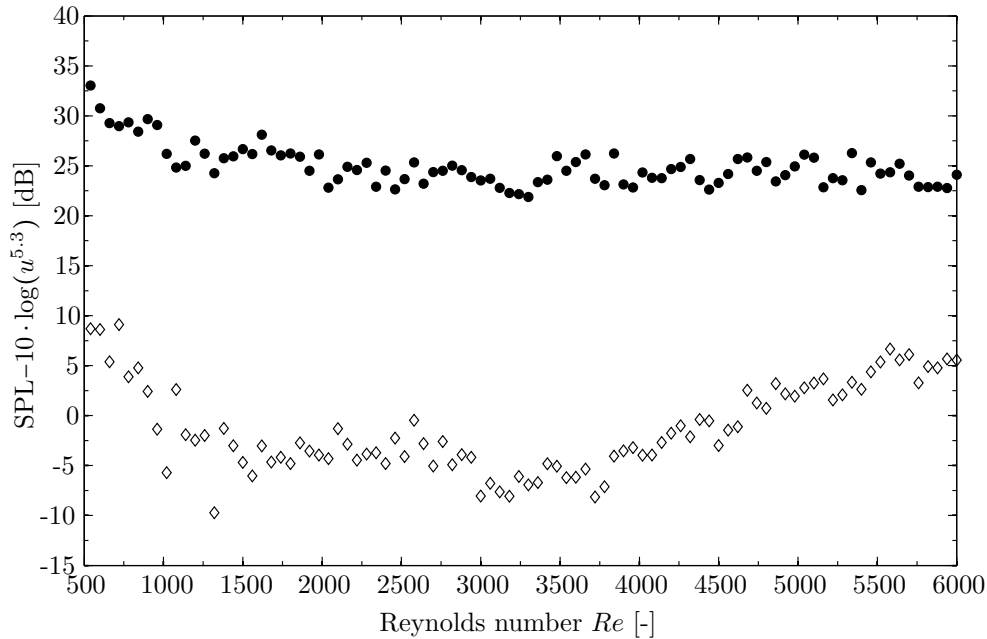


Figure 10. Sound pressure level of single cylinder  $\diamond$  and cylinder/plate-configuration  $\bullet$  at normalized distance  $g/d = 4$ , scaled to the 5.3 power of flow velocity  $u$ .

## Acknowledgments

The research project is part of the Competence Center Sound and Vibration Engineering (SAVE) founded by the Ministry for Innovation, Science and Research of the German federal state North Rhine-Westphalia. The first author would like to acknowledge the support by B.Virnich, Müller-BBM VibroAkustik Systeme GmbH for the measurement software PAK and the University of Adelaide for providing the test facilities.

## References

- <sup>1</sup>Brika, D.; Laneville, A., *The flow interaction between a stationary cylinder and a downstream flexible cylinder*, Journal of Fluids and Structures, Vol. 13, No. 5, 1999, pp. 579-606.
- <sup>2</sup>Carmo, B.S.; Meneghini, J.R.; Sherwin, S.J., *Possible states in the flow around two circular cylinders in tandem with separations in the vicinity of the drag inversion spacing*, Physics of Fluids, Vol. 22, 2010, Paper No. 054101.
- <sup>3</sup>Fey, U.; Koenig, M.; Eckelmann, H., *A new Strouhal-Reynolds-number relationship for the circular cylinder in the range  $47 < Re < 2 \times 10^5$* , Physics of Fluids, Vol. 10, Number 7, 1998, pp. 1547-1549.
- <sup>4</sup>Greschner, G.; Thiele, F.; Jacob, M.C.; Casalino, D., *Prediction of sound generated by a rod-airfoil configuration using EASM DES and the generalised Lighthill/FW-H analogy*, Computers & Fluids, Vol. 37, 2008, pp. 402-413.
- <sup>5</sup>Heckl, M., *Taschenbuch der technischen Akustik*, Berlin, Springer, 1975.
- <sup>6</sup>Jacob, M.C.; Boudet, J.; Casalino, D.; Michard, M., *A rod-airfoil experiment as benchmark for broadband noise modeling*, Theoretical Computational Fluid Dynamics, Vol. 19, 2005, pp. 171-196.
- <sup>7</sup>Kao, H.C., *Vortex/Body Interaction and Sound Generation in Low-Speed Flow*, National Aeronautics and Space Administration, Paper No. TM1998-208403, 1998.
- <sup>8</sup>Keefe, R.T., *An investigation of the fluctuating forces acting on a stationary circular cylinder in a subsonic stream, and of the associated sound field*, Institute of Aerophysics, University of Toronto (UTIA), Report No. 76, 1961.
- <sup>9</sup>Leehey, P.; Hanson, C.E., *Aeolian tones associated with resonated vibration*, Journal of Sound and Vibration, Vol. 13, 1971, pp. 465-483.
- <sup>10</sup>Liu, C.H.; Chen, J.M., *Observations of hysteresis in flow around two square cylinders in a tandem arrangement*, Journal of Wind Engineering and Industrial Aerodynamics, Vol. 90, 2002, pp. 1019-1050.
- <sup>11</sup>Norberg, C., *An experimental investigation of the flow around a circular cylinder: influence of aspect ratio*, Journal of Fluid Mechanics Fluid Mech, Vol. 258, 1994, pp. 287-316.
- <sup>12</sup>Norberg, C., *LDV-measurements in the near wake of a circular cylinder*, Advances in Understanding of Bluff Body Wakes and Vortex-Induced Vibration, Washington DC, 1998.
- <sup>13</sup>Norberg, C., *Fluctuating lift on a circular cylinder: review and new measurements*, Journal of Fluids and Structures, Vol. 17, 2003, pp. 57-96.

<sup>14</sup>Phillips, O.M., *The intensity of Aeolian tones*, Journal of Fluid Mechanics, Vol. 1, 1956, pp. 607-624.

<sup>15</sup>Roshko, A., *On the development of turbulent wakes from vortex streets*, NACA Rep. 1191, 1954.

<sup>16</sup>Singh, S.P.; Mittal, S., *Vortex-induced oscillations at low Reynolds numbers: Hysteresis and vortex-shedding modes*, Journal of Fluids and Structures, Vol. 20, No. 8, 2005, pp. 1085-1104.

<sup>17</sup>Tasaka, Y.; Kon, S.; Schouveiler, L.; Le Gal, P., *Hysteretic mode exchange in the wake of two circular cylinders in tandem*, Physics of Fluids, Vol. 18, 2006, Paper No. 084104.

<sup>18</sup>Wanderley, J.B.V.; Sphaier, S.H.; Levi, C., *A numerical investigation of the hysteresis effect on vortex induced vibration on an elastically mounted rigid cylinder*, Proceedings of the International Conference on Offshore Mechanics and Arctic Engineering - OMAE, Vol. 5, 2009, pp. 653-660.